







Sequential origin of an alternative colony founding strategy driven by two supergenes in *Temnothorax* ants

Hugo Darras ^{1,2*}, Chuanxin Yu ^{1,2}, Marion Kever ², Marah Stoldt ², Barbara Feldmeyer ³, Susanne Foitzik ²

¹Center for Evolutionary & Organismal Biology, School of Medicine, Zhejiang University, Hangzhou, China

²Institute of Organismic and Molecular Evolution, Johannes Gutenberg University, Mainz, Germany

³Senckenberg Biodiversity and Climate Research Center (SBIK-F), Molecular Ecology, Frankfurt, Germany

*Corresponding author: E-mail: hdarras@zju.edu.cn.

Associate editor: Russell Corbett-Detig

Abstract

Recent discoveries reveal that many complex intraspecific polymorphisms are shaped by a single supergene that maintains coadapted genetic variants through suppressed recombination. Here, we show that in the ant *Temnothorax rugatulus*, an extreme reproductive polymorphism is instead governed by two independent genomic rearrangements that arose sequentially on different chromosomes. Colonies of this species contain either a single large dispersing queen or multiple queens, including extremely miniaturized microgynes that cannot establish new colonies on their own and reproduce only by joining established multiple-queen colonies. Using chromosome-scale assemblies and population genomic data, we identify two genomic rearrangements, 9.3 and 7.0 Mb in size, that jointly determine these strategies. Divergence dating shows that the supergene underlying colony social structure arose first, creating the conditions for the subsequent emergence of a miniaturization supergene. These findings demonstrate that complex adaptive strategies can be assembled stepwise through the sequential origin of multiple supergenes.

Keywords supergene, social insects, complex traits, population genomics

Introduction

Colony-founding strategies and social organization display remarkable diversity across social insects (Wolf and Seppä 2016). In ants, the ancestral queen phenotype is a large, well-provisioned individual that disperses through nuptial flights and founds new colonies independently (monogynous colonies) (Boulay et al. 2014). However, dispersal is risky, with more than 99% of queens dying before reproducing (Wiernasz and Cole 1995). This cost is thought to have repeatedly favored the evolution of alternative reproductive behaviors in many species, with queens mating near their natal nests and reproducing after adoption into multi-queen colonies (polygynous colonies) (Keller 1995; Heinze and Keller 2000). Because these queens require fewer reserves, polygyny is often associated with reduced body size.

In some species, monogynous and polygynous nests coexist within populations. These alternative strategies were historically attributed to plastic responses to ecological conditions (Herbers 1986; Seppä et al. 1995; Ross et al. 1996; Banschbach and Herbers 1999; Pedersen and Boomsma 1999) but are now known to be often genetically controlled by large non-recombining supergenes

across diverse ant lineages (Kay et al. 2022; Chapuisat 2023), including *Solenopsis* fire ants (Wang et al. 2013; Helleu et al. 2022), several *Formica* species (Brelsford et al. 2020), *Cataglyphis niger* (Lajmi et al. 2026), *Myrmica ruginodis* (Sigeman et al. 2025), and *Myrmecina graminicola* (Mona et al. 2025). These supergenes differ in their mode of action but typically harbor a derived polygynous haplotype that alters queen morphology, physiology, and behavior (Ross and Keller 1995; Blacher et al. 2021), while in workers, this haplotype promotes acceptance of supernumerary queens (Keller and Ross 1998; Ross and Keller 1998; De Gasperin et al. 2025).

At the most extreme end of the spectrum of reproductive strategies observed in ants are microgynes, worker-sized queens whose reduced flight morphology precludes dispersal and whose adaptations for independent colony founding have been lost, such that they reproduce only through reintegration into existing colonies (Rüppell and Heinze 1999). In some species, all queens display this phenotype and live as interspecific social parasites, requiring the workers of a host species to establish their colonies before producing their own offspring (Buschinger 2009; Schär and Nash 2014; Leppänen et al. 2015; Dahan and Rabeling 2022). In others, two morphs of queens coexist within populations (Rüppell and Heinze 1999). In these species, microgynes

Received: October 19, 2025. **Revised:** March 31, 2026. **Accepted:** April 20, 2026

© The Author(s) 2026. Published by Oxford University Press on behalf of Society for Molecular Biology and Evolution.

This is an Open Access article distributed under the terms of the Creative Commons Attribution-NonCommercial License (<https://creativecommons.org/licenses/by-nc/4.0/>), which permits non-commercial re-use, distribution, and reproduction in any medium, provided the original work is properly cited. For commercial re-use, please contact reprints@oup.com for reprints and translation rights for reprints. All other permissions can be obtained through our RightsLink service via the Permissions link on the article page on our site—for further information please contact journals.permissions@oup.com.

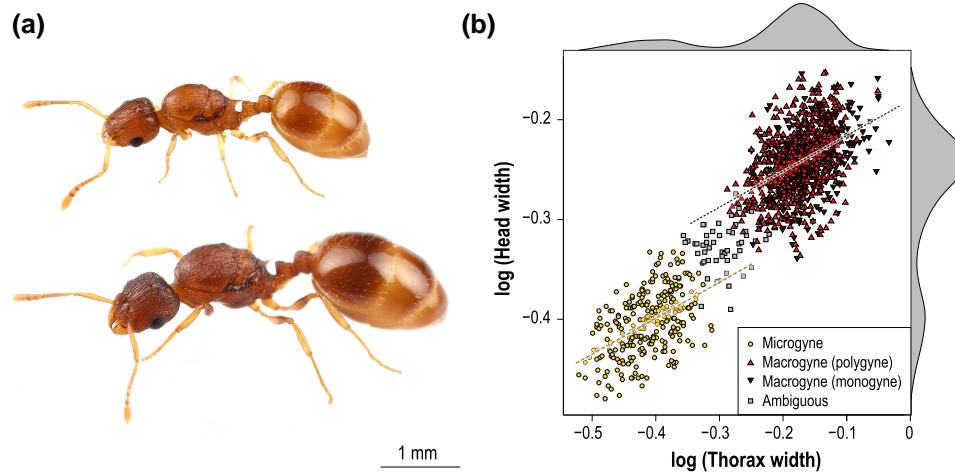


Figure 1 Distinct queen morphs in the ant *Temnothorax rugatulus* arise from different developmental programs. a) Photographs of microgyne (top) and macrogyne (bottom) queens, shown to scale. b) Log-transformed head width versus log-transformed thorax width for 1,350 queens (Negroni et al. 2021b), with regression lines for queens classified as microgyne, $\log(\text{head width}) = -0.254 + 0.362 \times \log(\text{thorax width})$, and macrogyne, $\log(\text{head width}) = -0.181 + 0.356 \times \log(\text{thorax width})$, based on body size index (Rüppell et al. 1998). No significant differences in intercept or slope were found between macrogyne from monogyne and polygyne colonies (ANCOVA, intercept: $df = 1,020$, $t = 1.328$, $P = 0.185$; slope: $t = 0.845$, $P = 0.398$). Square points indicate ambiguous morphologies.

adopt an alternative reproductive strategy by specializing in reintegration into their natal colony alongside closely related queens, an adaptation that promotes the colonization and monopolization of stable habitats (Wolf and Seppä 2016). The microgyne phenotype is associated with a suite of life-history traits, including colony-founding strategy and reduced dispersal, that depend on a polygynous colony structure in which workers tolerate supernumerary queens. In line with this, two recent studies in *F. cinerea* and *M. ruginodis* have identified genetic architectures underlying microgyne that are tightly linked to genetic polymorphisms controlling queen number (Scarpato et al. 2023; Sigeman et al. 2025). Because microgyne are unlikely to found colonies independently, polygyny is expected to be a prerequisite for the evolution of microgyne. However, the directionality of this association, that is, whether polygyny precedes and facilitates the evolution of microgyne or vice versa, has not yet been explicitly tested.

Here, we test the hypothesis that microgyne evolves as a secondary adaptation in lineages where polygyny has already arisen, by investigating the genetic basis of both queen-size dimorphism and polygyny in the North American *Temnothorax* (formerly *Leptothorax*) *rugatulus*. *Temnothorax rugatulus* is one of the best-studied ant species exhibiting size differences associated with distinct reproductive tactics in queens (Rüppell et al. 1998, Rüppell et al. 2001a, 2001b) (Fig. 1a). Large macrogyne queens typically found new monogyne colonies after mating flights, although some rejoin their natal colonies, resulting in polygyny. Smaller microgyne queens specialize in reintegration into established colonies, mostly their natal nest, and are therefore found predominantly in small polygyne associations of 2 to 3 related queens (Rüppell et al. 2001a). This contrasts with polygynous systems such as those of fire ants and *Formica* species mentioned earlier, where colonies contain large numbers of mostly unrelated queens. In *T. rugatulus*, both social organization and queen type are associated with distinct habitats. Monogynous colonies and macrogyne are more common in favorable, low-altitude environments, whereas polygynous

colonies and microgyne predominate in high-altitude, harsher habitats where independent colony founding is difficult (Heinze and Rueppell 2014; Choppin et al. 2021). Queen types differ not only in morphology and behavior but also in physiology; microgyne are more frequently fed by workers and exhibit an altered fat body gene expression and increased metabolic activity (Negroni et al. 2021b). Using a chromosome-scale genome together with resequencing, transcriptomics, and targeted genotyping in *T. rugatulus*, we demonstrate that microgyne is encoded by a large non-recombining haplotype that originated after the evolution of another non-recombining haplotype determining polygyny, thereby uncovering a stepwise trajectory in which successive genomic rearrangements shaped a novel queen founding strategy.

Methods

Sampling

All *T. rugatulus* used in this study were collected between 2015 and 2018 from a population in the Chiricahua Mountains (AZ, USA) (Choppin et al. 2021; Negroni et al. 2021b). Sequenced queens had previously been classified by Choppin et al. (2021) as microgyne or macrogyne using the size index of Rüppell et al. (1998), calculated from head width, thorax width, and thorax length. In that dataset, the bimodal distribution showed a minimum between the two modes at around 0.75. Queens with an index below 0.75 were therefore classified as microgyne, whereas those with an index of 0.75 or higher were classified as macrogyne (Table S6). Assignments were confirmed by visual inspection. We analyzed the genomes of 23 queens from different colonies sampled across five sites within an 11 km area (Figure S1 and Table S1). To assess genetic variation associated with queen morph, we compared eight macrogyne and eight microgyne from polygynous nests at four of the sites, with balanced sampling across morphs and sites. To assess genetic

variation associated with social structure, we analyzed seven additional macrogyne queens from monogynous nests at three sites, two of which overlapped with the sampling of polygynous nests (Figure S1). For this comparison, we retained only one of four queens from a polygynous site that was not represented among monogynous macrogyne, to limit potential effects of population structure (Table S1). To complement the genome analyses, we reanalyzed published transcriptomic data from queens (Negroni et al. 2019, 2021a, 2021b; Stoldt et al. 2025) and genotyped workers sampled from 42 colonies from the same population used for whole genome sequencing (Table S4).

Allometric relationships

Queen measurements were obtained from Negroni et al. (2021b). Queens were also classified using Ruppell's body size index. Because measurements in this dataset were shifted toward slightly higher values than in Choppin et al. (2021), we used a higher threshold than for the sequenced queens: queens with an index below 0.80 were classified as microgyne, whereas those with an index above 0.85 were classified as macrogyne. We verified bimodality in thorax width and thorax length using Hartigan's dip test for unimodality and Silverman's test for at most two modes (1,000 bootstrap replicates) implemented in the R packages *diptest* and *multimode*. To account for potential measurement error, we excluded individuals with outlier morphologies based on principal component analysis (PCA), defining outliers as those whose Mahalanobis distance from the mean exceeded the 90th percentile of the chi-squared distribution. Linear models were fitted to describe log-transformed head width as a function of log-transformed thorax width for each queen type, and differences in allometric relationships were assessed using analysis of covariance (ANCOVA).

Genome assembly and annotation

We assembled a de novo genome from a macrogyne monogyne colony using PacBio (non-HiFi) and Illumina reads (Jongepier et al. 2022). PacBio reads were assembled using Flye v2.9.4 (Kolmogorov et al. 2019) with the parameters “*-scaffold -iterations 1 -pacbio-raw*.” The resulting assembly was then polished using both Illumina and PacBio data with HyPo (Kundu et al. 2019). Haplotigs and contig overlaps were removed using *purge_dups* (Guan et al. 2020). Hi-C data (16.57 Gb) were obtained from a single macrogyne monogyne queen using the Arima-high coverage kit. The Hi-C reads were aligned to the draft genome using Juicer (Durand et al. 2016), and scaffolding was performed using the 3D-DNA pipeline with parameters “*-r 6 -polisher-input-size 10,000 -splitter-input-size 10,000*” (Dudchenko et al. 2017). The candidate assembly was manually reviewed and polished using Juicebox (Durand et al. 2016). Gap closure was then performed using PacBio reads with TGS-GapCloser (Xu et al. 2020), followed by a final polishing round with HyPo. We used BUSCO v5.4.3 (Simão et al. 2015) with the *hymenoptera_odb10* single-copy ortholog database to monitor assembly completeness at each step. Annotations were transferred from a prior draft assembly (Vizueta et al. 2025) using LiftOff (Shumate and Salzberg 2021).

Population genetics

DNA was extracted from queens without gasters, and libraries were sequenced as 150 bp paired-end lanes (NovaSeq X Plus, Novogene). Reads were aligned with BWA v0.7.17 (Li and Durbin 2009), variants were called with FreeBayes v1.3.6 (Garrison and Marth 2012) with clustering disabled, and unplaced contigs were excluded. Variants were filtered with VCFtools v0.1.16 (Danecek et al. 2011) (–min-meanDP 7, –max-meanDP 27, –minQ 20, –remove-indels, –min-alleles 2, –max-alleles 2). F_{ST} was computed in 100 kb nonoverlapping windows with *popgenWindows.py* from S. Martin's *genomics_general* repository (–w 100,000 –s 0 –windType coordinate –ploidy 2 –f phased). Individuals were grouped by morph and social form (Table S1). Heterozygosity was calculated using VCFtools and measured as the percentage of polymorphic positions that were heterozygous per individual. PCA for subregions was performed using the R package *SNPRelate* (Zheng et al. 2012). For linkage disequilibrium, we removed sites with missing genotypes in more than one sample and thinned to one single nucleotide polymorphism (SNP) per 15 kb. Linkage disequilibrium was computed with PLINK v1.9 (Chang et al. 2015) as pairwise r^2 within 40 Mb (–ld-window 40,000,000, –ld-window-kb 40,000). To enable PLINK to handle non-recombining blocks lacking 1/1 genotypes, we added an artificial 1/1 sample at every position in the VCF.

Genotyping

We designed two multiplex PCR assays diagnostic for NR8 and NR2 haplotypes. Short genomic segments with < 50 bp size differences were identified in resequenced queens; indels were called with FreeBayes and phased with WhatsHap (Martin et al. 2023). Assay 1 targets three biallelic markers for S and L plus one triallelic marker for S, L1, and L2. Assay 2 targets three biallelic markers for M and P (Table S7). DNA was extracted with 5% Chelex; PCR was performed using QIAGEN Multiplex Master Mix, with 35 cycles and 62 °C annealing. Fragment sizes were scored with STRyper (Peccoud 2025).

Analyses of transcriptomic data

Published RNA-seq was reanalyzed as follows: reads were aligned with STAR v2.7.8 (Dobin et al. 2013), variants were called with FreeBayes (–min-repeat-entropy 0, –limit-coverage 50, –use-best-n-alleles 4) and filtered with VCFtools (–mac 3, –remove-indels, –min-alleles 2, –max-alleles 2). Haplotypes in NR8 and NR2 were assigned based on diagnostic SNPs. To assess variation on chromosome 4 (see Results), we performed an additional F_{ST} analysis based on transcriptomic data from 22 monogyne macrogyne and 25 polygyne macrogyne (see Figure S2 and Table S2). For this analysis, we applied more stringent variant filtering to reduce noise associated with SNP calling from transcriptomic data (–mac 5, –minQ 30, –max-missing 0.8). The F_{ST} plot was generated following the same procedure described above.

Dating

We estimated the relative ages of the M/P, S/L, and L1/L2 rearrangements using divergence at fourfold (4D) degenerate sites in heterokaryotypes, assuming similar ancestral polymorphism

and negligible recombination between supergene haplotypes. Age estimates were calculated using the formula $(D_{\text{rearrangement}} - D_{\text{background}})/(2\mu)$, where $D_{\text{rearrangement}}$ is the average 4D divergence within the rearrangement, $D_{\text{background}}$ represents contemporary genome-wide 4D divergence between a queen's parental haplotypes (excluding non-recombining regions), and μ is the per-generation mutation rate in Hymenoptera (3.5×10^{-9}), based on substitution rates in *Apis* (Yang et al. 2015) and *Bombus* (Liu et al. 2017). We assumed a generation time of 6 to 8 years, given that queens of the congeneric *Temnothorax nylanderii* can live up to 20 years (Plateaux 1986) and that both microgynes and macrogynes of *T. rugatulus* have been maintained in our laboratory for over 8 years.

Synteny analyses

We aligned the genome of *T. rugatulus* to those of the ants *Solenopsis invicta* (GCF_016802725), *Formica selysi* (GCA_009859135), *Myrmica ruginodis* (kindly provided by H. Sigeman), *Myrmecina graminicola* (GCA_976941435.1), *Pogonomyrmex californicus* (GCA_050084945.1) and *Cataglyphis niger* (GCA_050437125) using minimap2 v2.29 (Li 2018) with the parameter set `-x asm5`. Alignments shorter than 5 kb were discarded, and synteny was visualized using Circos v0.69-8 (Krzywinski et al. 2009).

Results

Two distinct queen developmental trajectories in *T. rugatulus*

Queens of *T. rugatulus* occur as macrogynes or microgynes, corresponding to bimodal distributions of representative body measurements like thorax width and length (Hartigan's dip test, both $P < 0.001$; Silverman test, both $k = 2$, $P > 0.2$), suggesting different investment in flight musculature. To evaluate whether these morphs represent discrete phenotypic states or the extremes of a continuous distribution shaped by environmental and social factors, we examined the allometric relationship between log-transformed head and thorax widths (Fig. 1b). Slopes did not differ between morphs (ANCOVA: $df = 1296$, $t = 0.131$, $P = 0.895$), but intercepts did ($t = -4.373$, $P = 1.32e-05$), supporting the interpretation that macrogynes and microgynes arise from distinct developmental trajectories (Wheeler and Nijhout 1983; Rajakumar et al. 2018).

Two supergenes on different chromosomes control queen morphology and colony structure

Previous mother-offspring comparisons suggested that queen-size dimorphism in *T. rugatulus* has a heritable component (Rüppell et al. 2001b). To help resolve the genomic bases of queen traits, we assembled a high-quality genome for the macrogyne monogyne form using PacBio, Illumina, and Hi-C data. The new 329 Mb assembly recovered more than 96% of conserved single-copy Hymenoptera orthologs, anchored

92% of the sequence to 14 chromosome-scale scaffolds consistent with the species' known karyotype (Crozier 1970), and clearly delineated the two arms of most chromosomes (Fig. 2a–c).

To identify genomic determinants of queen size, we analyzed 16 genomes from macrogynes and microgynes co-occurring within the same population, sampled on the eastern and western slopes of the Chiricahua Mountains (Table S1 and Figure S1). Differentiation between the two morphs, estimated across the entire genome, was low ($F_{ST} = 0.004$), consistent with ongoing gene flow. Elevated F_{ST} was limited to a single 7.0 Mb region on the 5' arm of chromosome 8 (0 to 7,015,000 bp; 344 annotated genes), hereafter NR8 (Non-Recombining Region 8; Fig. 2d). NR8 harbors 51,486 SNPs in strong linkage disequilibrium away from the centromeric region, consistent with a genomic rearrangement, for which one or more large inversions could provide a plausible explanation (Fig. 2b). A PCA of NR8 resolved two clusters along PC1 with contrasting heterozygosity and corresponded to different combinations of two non-recombining haplotypes, which we named L and S based on their association with queen size (Large and Small). The first cluster comprises an L/L homokaryotype and is formed exclusively by the eight sequenced macrogynes, whereas the second cluster comprises an S/L heterokaryotype and includes only the eight microgynes (Fig. 2f). PC2 further subdivided samples into a 2.8 Mb subregion (0 to 2,850,000 bp; 158 genes) with two non-recombining L haplotypes, L1 and L2. Both haplotypes occurred in macrogynes (L1/L1, L1/L2, L2/L2) and microgynes (S/L1, S/L2). We hereafter refer to L1 and L2 collectively as L, as we have yet not found evidence that they differ in their association with any phenotype. Overall, NR8 represents a large block of suppressed recombination, or supergene, in which the likely derived S haplotype acts dominantly and is both necessary and sufficient for the development of the microgyne phenotype, thus connecting this genomic region to queen-size dimorphism in *T. rugatulus*.

In *T. rugatulus*, microgynes are strongly linked to polygyny, but polygyny also appears without microgynes. To assess whether social form has a distinct genetic basis, we compared the genomes of 12 macrogynes from monogyne and polygyne colonies from the same population (Table S1). Genome-wide F_{ST} between the two colony types was again low (0.010), yet a 9.3 Mb region on the 3' arm of chromosome 2 (17,780,000 to 27,083,407 bp; 511 genes), hereafter NR2, showed strong F_{ST} (Fig. 2e). NR2 spans 79,684 SNPs in strong linkage disequilibrium, indicative of an underlying genomic structural change (Fig. 2c). PCA of this region revealed two clusters that differ in heterozygosity and correspond to two non-recombining haplotypes, M and P (for monogyne and polygyne). These haplotypes form two main genotypes: an M/M homokaryotype found only in the sequenced queens from monogyne colonies, and an M/P heterokaryotype present in sequenced queens from polygyne colonies (Fig. 2g). A weaker F_{ST} signal in the pericentromeric region of chromosome 4 did not segregate clearly with social form, suggesting sampling noise (Figure S2). However, in the absence of a Hi-C reference assembly for P/P individuals, we cannot exclude that this signal reflects an interchromosomal rearrangement involving the P haplotype. Overall, these analyses identified NR2 as a large non-recombining region underlying variation in colony queen number

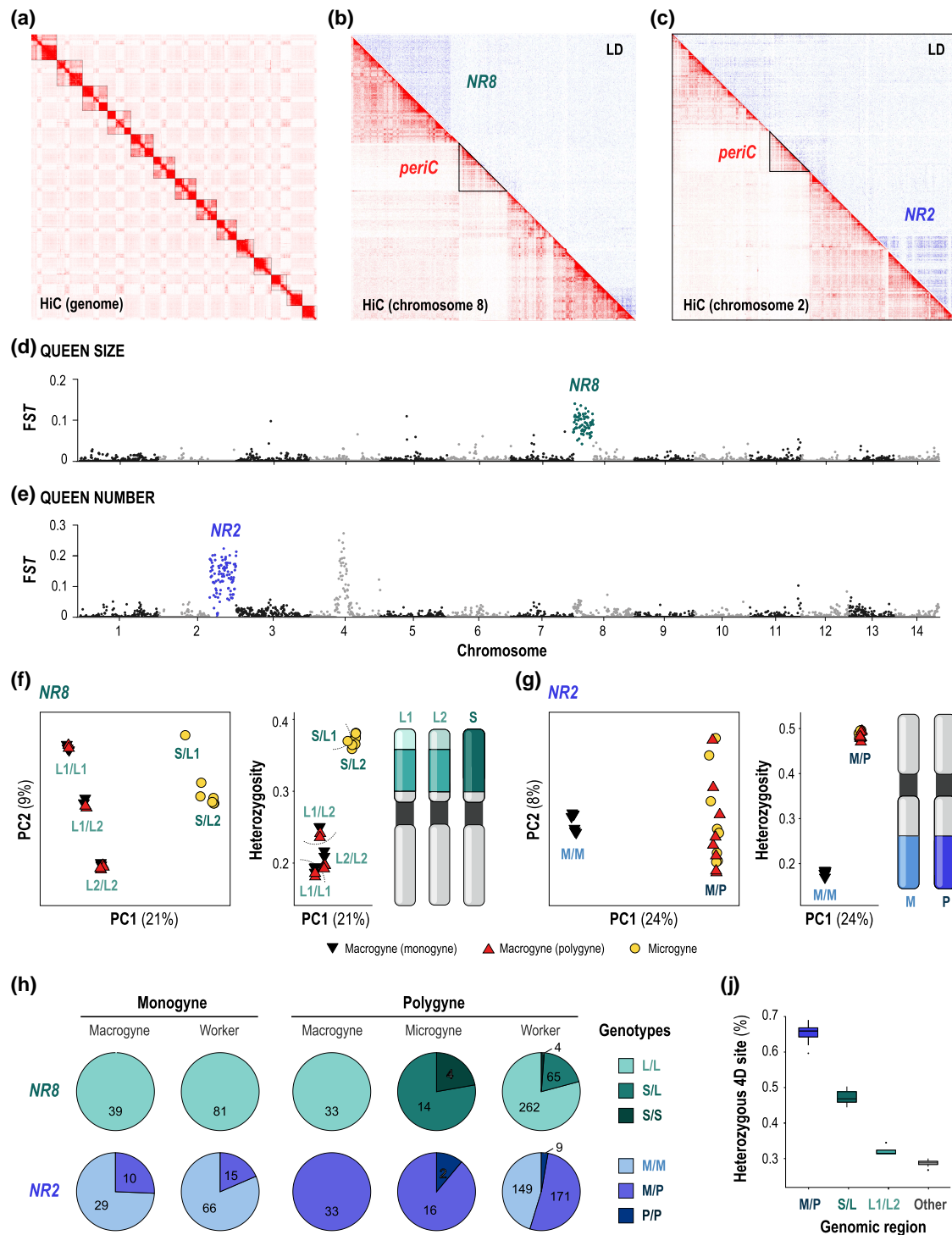


Figure 2 Genomic basis of queen size and colony queen number. a) Hi-C contact map of the 329 Mb *T. rugatulus* genome showing 14 chromosome-scale scaffolds. The color scale represents interaction frequencies. b–c) Hi-C contact and linkage disequilibrium (LD) heatmaps for chromosomes 8 and 2, highlighting NR8 and NR2. Pericentromeres (periC) are marked. d) Genome-wide F_{ST} between 8 macrogyne and 8 microgyne, with a peak at chromosome 8 (NR8). e) Genome-wide F_{ST} between 7 monogyne macrogyne and 5 polygyne macrogyne, with a peak at chromosome 2 (NR2). A secondary peak on chromosome 4 (8,525,000 to 14,585,000 bp) does not track social form (Figure S2). f) PCA and heterozygosity for 51,486 polymorphic sites on NR8 (chromosome 8: 0 to 7,015,000 bp); schematic of the putative rearrangements separating the S, L1, and L2 haplotypes. g) PCA and heterozygosity for 79,684 polymorphic sites on NR2 (chromosome 2: 17,780,000 to 27,083,407 bp); schematic of the putative rearrangement separating the M and P haplotypes. h) Pie charts of NR8 and NR2 genotypes from 16 queen whole genomes, 67 queen RNA-seq, and 412 worker genotyping (two with missing data for NR2). Among 343 workers with the L/L karyotype at NR8, genotype frequencies were 27% L1/L1, 35% L1/L2, and 38% L2/L2 (Table S4), indicating a balanced polymorphism of L variants. i) Divergence at 4D sites in heterokaryotypes: M versus P ($N = 16$ M/P), S versus L ($N = 8$ S/L1 or S/L2), and L1 versus L2 ($N = 4$ L1/L2). Background heterozygosity was calculated genome-wide for 23 queens, excluding NR8 and NR2.

in *T. rugatulus*, with a dominant and putatively derived P haplotype required for the expression of polygyne traits.

Rare homozygosity for derived supergene haplotypes reflects low frequencies or fitness of male carriers

New rearranged haplotypes often persist at low frequency and are therefore rarely found in the homozygous state, which allows recessive deleterious alleles to accumulate under suppressed recombination (Faria and Navarro 2010). Accordingly, in many supergene systems, homozygosity for derived haplotypes is lethal (Kay et al. 2022). We therefore asked whether the S and P haplotypes occur as homozygotes in nature, given that the whole-genome sequencing described above detected them only in the heterozygous state. We augmented our dataset with transcriptomes from mated queens from 67 additional colonies (Table S2) (Negroni et al. 2019, Negroni et al. 2021a, 2021b; Stoldt et al. 2025). With this larger sampling, all three female karyotypes were detected for each rearrangement (S/S, S/L, L/L for NR8; M/M, M/P, P/P for NR2). The S haplotype at NR8 was found only in queens that also carried the P haplotype at NR2, but the two regions were not genetically linked. Specifically, the frequency of M/P individuals did not differ between S/L and S/S queens ($\chi^2 = 1.00$, $P = 0.32$; Yates-corrected $\chi^2 = 0.01$, $P = 0.92$), consistent with the Hi-C contact map showing that NR2 and NR8 segregate on different chromosomes (Fig. 1a). In line with previous results, all microgynes carried at least one S haplotype, either S/L or S/S, with S/S being less frequent (22% of microgynes, including whole genome sequenced individuals; Fig. 2h), whereas all macrogynes were L/L (Fisher's exact test for presence of S, $P < 2.2 \times 10^{-16}$). Micro- and macrogynes from polygyne colonies always carried at least one P haplotype, most commonly M/P (96%) and more rarely P/P. In colonies recorded in the field as monogyne, the P haplotype was, as expected, less frequent (74% M/M and 26% M/P; Fisher's exact test for presence of P, $P = 1.92 \times 10^{-15}$). The presence of P carrying queens in monogynous colonies may reflect nests that were formerly polygynous but experienced recent queen loss, or nests in which additional queens were missed during field sampling. Overall, these data indicate that S/S and P/P queens, as well as the S- and P-haplotype males that must have sired them, are at least partially viable. Queens homozygous for the derived NR8 S haplotype and the NR2 P haplotype were nevertheless detected only at low frequency. One possible explanation is that S and P alleles are rare in males.

Because ant males develop from unfertilized eggs, S-haplotype males can only be produced by S-carrying microgynes, whereas P-haplotype males are expected mainly from polygyne colonies. In the Chiricahua Mountains, both polygyne nests and microgynes are uncommon (34% polygyne nests with a mean of 20% microgynes) (Negroni et al. 2021b). Using these values together with queen genotype frequencies estimated from our study, we inferred the haplotype frequencies among males expected to be produced each year (Table S3). Assuming that colonies of different types produce equal numbers of males and that queens within colonies contribute equally, 6% of all males produced are expected to carry the S haplotype at

NR8, and independently, 27% to carry the P haplotype at NR2. While the relatively low allele frequency of S may account for the rarity of S/S queens, the expectation that approximately one quarter of males carry the P haplotype contrasts with the observation that only 4% of queens are homozygous P/P.

To gain insight into the distribution of the S and P haplotypes in the population, we extended genotyping to worker females, which are expected to more accurately reflect patriline frequencies than queens, as queens are likely to be subject to strong genotype-dependent selection pressures. In total, we genotyped 412 workers from 9 monogyne and 33 polygyne colonies using multiplex PCR assays for both loci (Tables S4–S5). As expected, no linkage between the NR8 and NR2 rearrangements was detected: among S/L workers, 40% were M/M and 60% were M/P.

As in queens, the S haplotype occurred at low frequency among workers. Among the offspring of macrogyne queens, the S haplotype was absent in workers from monogyne colonies and present in only 5% of workers from polygyne colonies (Fig. 2h), consistent with the expectation that only 6% of males carry the S haplotype. In polygyne colonies containing only S-carrying microgynes, 56% of workers carried the S haplotype, but only 3% ($N = 1$) were S/S, as expected if most mating occurs with L-carrying males (Table S4). Altogether, these results confirm that the S haplotype is maintained at low frequency in the population, with no detectable evidence for strong fitness costs of the homozygous genotype given the available data.

We next examined worker genotypes at the NR2 polymorphism, for which the P haplotype is relatively frequent among queens but rarely observed in the homozygous state. In monogynous colonies, P occurred in 19% of workers but was never detected as P/P (Fig. 2h). When present, M/P workers always co-occurred with M/M nestmates (Table S4), a pattern consistent with inheritance of the P haplotype from a formerly polygynous M/P queen that mated with an M male. This interpretation assumes single mating, which appears to be the rule in this ant clade (Boomsma et al. 2009), and suggests that mating with P males is rare. Similarly, in polygynous colonies, where all queens carried the P haplotype, only 3% of workers were P/P homozygotes (Fig. 2h). This contrasts with the expectation that one quarter of males carry the P haplotype, which under random mating would result in substantially higher frequencies of P/P workers in polygynous colonies. This pattern again supports the conclusion that mating with P males is uncommon.

An alternative explanation for the scarcity of P/P workers is partial deleteriousness of the P haplotype in the homozygous state, as often observed for derived supergene haplotypes (Jay et al. 2021; Blacher et al. 2023). To test this hypothesis explicitly, we estimated the frequency of matings between polygynous queens and P males based on the observed distribution of M/M, M/P, and P/P genotypes among worker offspring (Supplementary Text S1). Worker data were best explained by a model in which 4% of queens in polygynous colonies were P/P, consistent with direct queen genotyping, and only 5% of queen matings involved P males (log-likelihood = -262.32 , AIC = 528.63). Allowing for reduced viability of P/P workers did not improve model fit (log-likelihood = -262.32 , AIC = 530.63; likelihood ratio test, $P = 1$). These results indicate that P/P mortality is unlikely to be the primary cause of the observed deficit and instead suggest that mating with P males occurs less frequently than expected.

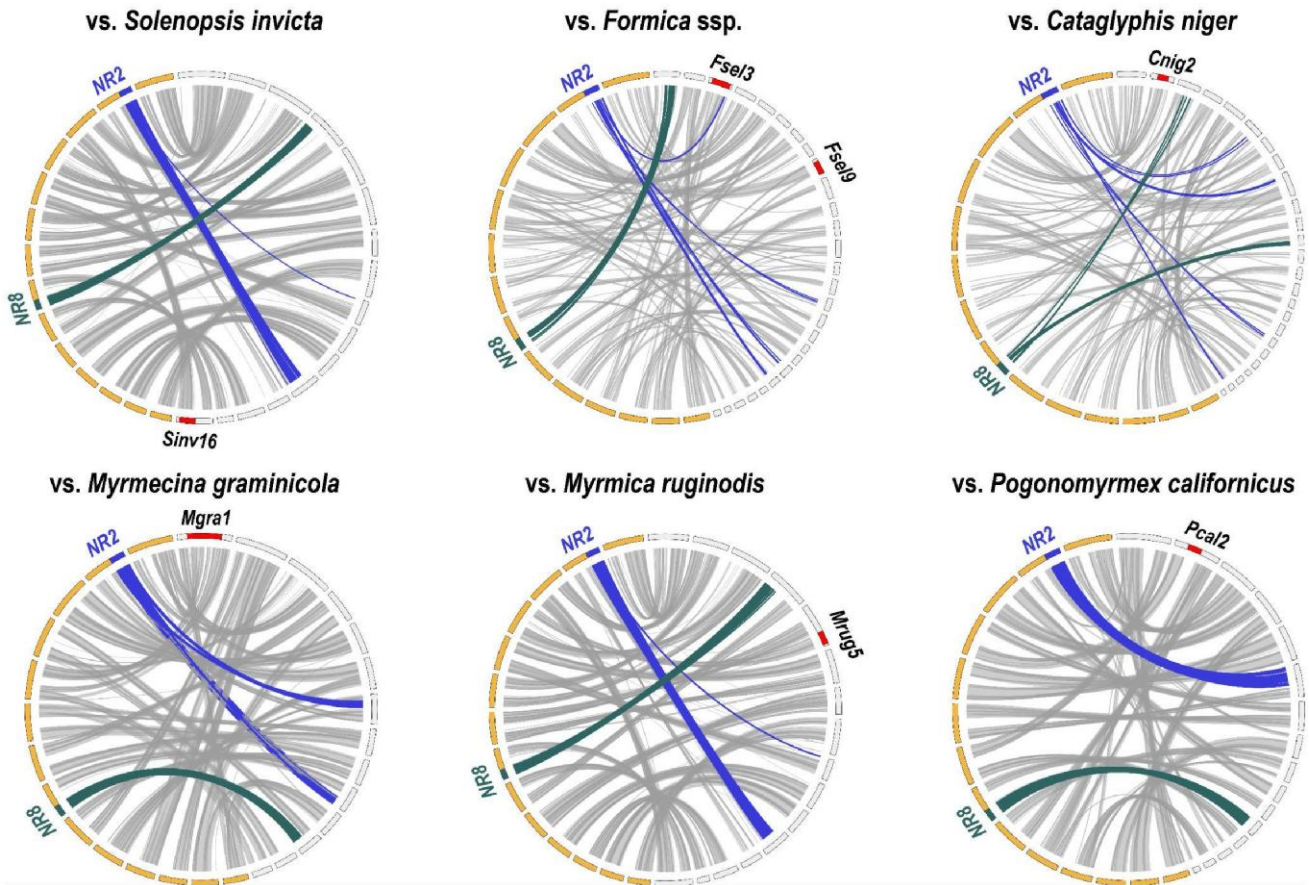


Figure 3 Genome synteny between *Temnothorax rugatulus* and other ant species with supergenes controlling queen number, queen morphology, or founding strategy. Each synteny plot shows pairwise alignments between *T. rugatulus* (left, yellow) and a target species (right, gray). Each box represents a chromosome or scaffold. Blue and green boxes indicate the locations of the supergenes identified in *T. rugatulus*, while red boxes indicate supergenes identified in the target species. Shown are *Sinv16* (chromosome 16), which controls queen number in *Solenopsis invicta* (Wang et al. 2013); *Fsel3*, which controls queen number in *Formica selysi* and other *Formica* species (Brelford et al. 2020); *Fsel9*, which controls queen size in *Formica cinerea* (Scarpato et al. 2023); *Cnig2*, which controls queen number in *Cataglyphis niger* (Lajmi et al. 2026); *Mgra1*, which controls queen size and number in *Myrmecina graminicola* (Mona et al. 2025); *Mrug5*, which controls queen size and number in *Myrmica ruginodis* (Sigeman et al. 2025); and *Pcal2*, which controls queen founding strategy in *Pogonomyrmex californicus* (Errbii et al. 2024), is also shown. For *P. californicus*, we performed mapping onto the updated genome assembly GCA_050084945.1. Gray links indicate genome wide synteny; green links connect the *T. rugatulus* NR8 region associated with queen size to homologous regions in the other species, and blue links connect the NR2 region associated with queen number.

The NR8 miniaturizing supergene arose after the NR2 supergene underlying polygynous social organization

Polygyny in ants evolved secondarily from monogynous ancestors (Boulay et al. 2014). In *T. rugatulus*, microgyny is consistently associated with traits of the polygyny syndrome, including short-range dispersal and cooperative colony founding (Wolf and Seppä 2016). We therefore hypothesized that polygyny evolved before microgyny in this species. Divergence at fourfold degenerate sites in heterokaryotypes showed exactly that. The M/P rearrangement predates the S/L rearrangement, and divergence between the L1 and L2 haplotypes within L is only marginally above background levels (Fig. 2j). Using the mutation rate estimated in bees (Yang et al. 2015; Liu et al. 2017), we estimate that the P haplotype originated approximately 517,000 generations ago, the S haplotype about 260,000 generations ago, and

the L1/L2 haplotypes about 48,000 generations ago. Assuming a generation time of 6 to 8 years, the oldest P rearrangement haplotype likely originated a few million years ago, probably after *T. rugatulus* diverged from its closest relatives (Prebus 2017). These estimates are inherently approximate, as they assume ancestral polymorphism similar to present levels and negligible recombination or gene conversion.

The NR8 and NR2 supergenes are unrelated to previously described ant supergenes

In ants, the first two supergenes identified as controlling queen number, in *S. invicta* and *F. selysi*, showed no homology, suggesting convergent evolution of distinct genomic architectures (Purcell et al. 2014). More recently, a supergene controlling


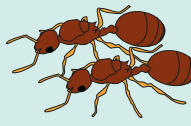



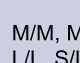

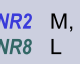
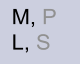
	MONOGYNE COLONIES	POLYGYNE COLONIES (determined by haplotype P)	
	MACROGYNE	MACROGYNE	MICROGYNE (determined by haplotype S)
QUEENS	 NR2 M/M NR8 L/L	 NR2 M/P, P/P NR8 L/L	 NR2 M/P, P/P NR8 S/L, S/S
DAUGHTERS	 NR2 M/M, M/P? NR8 L/L, S/L?	 NR2 M/M, M/P, P/P NR8 L/L, S/L	 NR2 M/M, M/P, P/P NR8 L/L, S/L, S/S
SONS	 NR2 M NR8 L	 NR2 M, P NR8 L	 NR2 M, P NR8 L, S

Figure 4 Genetic composition of different colony types in *T. rugatulus*. Genotype composition at the social supergene (NR2) and the queen morph supergene (NR8) in mother queens, their female offspring (fertilized eggs that develop into queens and workers), and their male offspring (unfertilized haploid eggs). Only monogynous colonies assumed to have been founded independently are shown. Queens carrying the P haplotype were occasionally observed in monogyne colonies, but we suspect that these cases reflect queens originating from former polygyne colonies. Rare genotypes are indicated in gray, and genotypes marked with question marks were not observed but are theoretically possible.

queen number in *C. niger* was found to be homologous to that of *S. invicta* (Lajmi et al. 2026). These two ant species diverged more than 90 million years ago, yet their supergene locations largely overlap. To assess whether the two supergenes in *T. rugatulus* share homology with previously described ant supergenes, we performed whole genome alignments with the genome assemblies of all six genera, in which supergenes have been reported. We detected no homology with any of these supergenes, with the exception of *F. selysi* (Fig. 3). In this species, homology was limited to a single 450 kb region of NR2 that overlaps with the queen number supergene and contains only 19 genes (Table S5).

Discussion

Our results show that in *T. rugatulus*, extremely miniaturized microgynes, which mostly occur in colonies with multiple queens, are associated with variation at two large, independent supergenes NR8 and NR2 (Fig. 4). The supergene on chromosome 2 is strongly associated with colony social structure, showing a biased distribution between single-queen and multiple-queen colonies, while the supergene on chromosome 8 is associated with queen size. Together, these two genomic regions are linked to one of the most extreme reproductive strategies described in ants, in which worker-sized queens forego dispersal and reproduce exclusively within established multiple-queen colonies.

The P haplotype on chromosome 2 likely influences both queen dispersal behavior and the acceptance of additional queens by workers as described in *Solenopsis* and *Formica* ants (Keller and Ross 1998; Ross and Keller 1998; De Gasperin et al. 2025). However, because polygyne colonies of *T. rugatulus* contain only a few, closely related queens, we propose that this polygyne supergene operates differently from the well-studied selfish supergene of *Solenopsis*, which promotes the coexistence

of large numbers of unrelated queens carrying the polygyne haplotype.

P-carrying queens were occasionally found heading colonies alone. We hypothesize that this pattern reflects the misclassification of colonies as having been founded by a monogynous queen. This interpretation is particularly plausible given that approximately 30% of polygynous *T. rugatulus* nests contain only two queens and could therefore be readily misclassified if sampling is incomplete. Moreover, queens were not detected in 17% of all sampled nests, indicating that queen loss is frequent in this species (Negroni et al. 2021b). Similar mismatches between the presence of a polygyne-associated haplotype in queens and an inferred monogynous social organization have recently been reported in three other ant species and were likewise attributed to recent queen loss (Scarpato et al. 2023; Mona et al. 2025; Sigeman et al. 2025). At the same time, these observations remain compatible with a scenario in which the P haplotype reduces, but does not completely eliminate, the likelihood of independent colony founding, for example if its effects are mediated primarily through workers rather than acting as an absolute constraint on queen behavior. Such partial uncoupling between genotype and behavior has been documented in *S. invicta*, where queens lacking the polygyne-associated haplotype occasionally exhibit behaviors typical of polygyne queens, including attempts to enter established nests and initiate egg laying in the presence of workers (Vaughn et al. 2025).

The distribution of genotypes at the queen number NR2 polymorphism showed an excess of M/M and M/P worker genotypes in polygynous colonies relative to Hardy–Weinberg expectations. Our analyses suggest that this pattern is best explained by a reduced contribution of P males to mating. One possible explanation is that P males have lower fitness than M males because purifying selection is less effective on the P haplotype, which experiences reduced recombination and a smaller effective

population size (Küpper et al. 2016; Blacher et al. 2023). Consistent with this hypothesis, males carrying the derived social chromosome in socially polymorphic *Solenopsis* and *Formica* ants exhibit reduced fertility (Lawson et al. 2012; De Gasperin et al. 2025). Alternatively, P males may experience reduced mating opportunities due to female mating biases favoring M genotypes (Avril et al. 2019; Walker et al. 2025).

The S haplotype on chromosome 8 appears to influence queen development, producing individuals that are nearly worker sized. In parallel with our work, supergene-mediated reductions in queen dispersal ability through changes in body size or wing loss have recently been reported independently in *Formica cinerea* (Scarparo et al. 2023), *M. graminicola* (Mona et al. 2025), and *M. ruginodis* (Sigeman et al. 2025). In *M. graminicola* and *M. ruginodis*, this is associated with a single genomic region, while in *F. cinerea* two regions are consistently coinherited, although it remains unclear whether the latter are physically linked. In *T. rugatulus*, by contrast, microgynes were associated with haplotypes at two large regions that segregate independently on different chromosomes. Microgynes carrying the S haplotype in the absence of the P haplotype were not observed, suggesting that the S haplotype without P either does not permit queen development or produces a maladaptive queen phenotype combining dispersal behavior with non-dispersing morphology, leading to low survival and colony-founding success. The S haplotype was rare, consistent with the low frequency of the microgyne phenotype in the studied population, and our sampling did not reveal a lower frequency of S/S genotypes or S males than expected, although larger sample sizes will be required to validate this conclusion.

We acknowledge that genotyping adult individuals sampled in the field cannot capture the full biological complexity of such systems, and that our inferences on mating patterns should therefore be regarded as preliminary. In the two best studied ant supergene systems to date, *S. invicta* and *F. selysi*, detailed biological work has revealed processes that strongly bias genotype representation within colonies. In *S. invicta*, the derived polygyne haplotype induces workers to eliminate non-carrier queens, leading to its overrepresentation among surviving queens (Keller and Ross 1998), whereas in *F. selysi*, the P haplotype acts as a maternal effect killer, preventing the hatching of M and M/M eggs laid by M/P queens (Avril et al. 2020). The strikingly different modes of action uncovered in these two systems suggest that ant supergenes encompass a broader diversity of biological mechanisms, many of which are likely to be discovered through further study of additional systems such as that of *T. rugatulus*.

Divergence dating indicates that the supergene underlying colony social structure arose before the miniaturization supergene. This temporal sequence supports the hypothesis that the evolution of multiple queen colonies created ecological and social conditions that favored the subsequent emergence of specialized microgynes. A similar scenario has been proposed in *F. cinerea*, where a rearrangement associated with social structure appears to have expanded to include an additional non-recombining region affecting queen size, although the relative timing of the origin of this size polymorphism has not yet been evaluated (Scarparo et al. 2023). Interestingly, in *M. graminicola*, social structure and queen morphology likewise arose through successive genomic rearrangements, but divergence dating

suggests that, in this species, the polymorphism encoding queen size predates that associated with social structure (Mona et al. 2025). Together, these results point to a reciprocal, reinforcing process in which supergene-mediated changes in either social structure or queen morphology alter the selective context in ways that facilitate the subsequent emergence of rearrangements affecting the complementary trait. Such feedback between social organization and morphology provides a route for the evolution of increasingly integrated reproductive strategies.

Our analyses uncovered a third, more recent layer of variation within the ancestral queen-size L haplotype, where two smaller haplotypes, L1 and L2, are maintained despite showing no obvious association with queen morphology or social form. Because ant species typically have small effective population sizes, in which neutral variants are expected to drift to fixation or loss (Romiguier et al. 2014), the maintenance of both haplotypes at high frequencies is consistent with an adaptive polymorphism whose selective basis remains unresolved.

Taken together, our results show that complex, supergene-mediated, adaptive polymorphisms need not be controlled by a single locus. In *T. rugatulus*, an extreme reproductive strategy evolved stepwise through the sequential emergence of two supergenes on different chromosomes, illustrating how structural genomic rearrangements can interact to generate novel adaptations.

Acknowledgments

We thank M. Litto for laboratory management; J. Hirsch and M. Halir for DNA extractions; M. Choppin and M. Negroni for sample information; the Senckenberg NGS facility for Hi-C preparation; Novogene for Illumina sequencing; H. Sigeman and L. Viljakainen for providing the *Myrmica* genome; Q. Pan, T. J. Colgan, and G. Scarparo for feedback on analyses and results; and C. Doums for extensive comments that improved the manuscript.

Supplementary material

Supplementary material is available at *Molecular Biology and Evolution* online.

Funding

This research was supported by grants from the German Research Foundation (DFG; HD: DA 2890/2-1 and SF: Fo FG FO 298/19–1/2 (research unit FOR-228) and GRK2526/1).

Conflicts of interests

The authors declare no competing interests.

Data availability

All data are available in the paper and [Supplementary Materials](#). Sequencing reads have been deposited in NCBI (PRJNA1328983) and are available for reviewers at the following link: <https://>

dataview.ncbi.nlm.nih.gov/object/PRJNA1328983?reviewer=hjh0mfo7s8bab0mgf6s1g2m1lb. The genome assembly is available under BioProject PRJNA1328450. Command lines required to replicate all analyses are provided as a Supplementary file.

References

- Avril A, Purcell J, Béniguel S, Chapuisat M. Maternal effect killing by a supergene controlling ant social organization. *Proc Natl Acad Sci U S A*. 2020;117:17130–17134. <https://doi.org/10.1073/pnas.2003282117>.
- Avril A, Zahnd S, Djordjevic J, Chapuisat M. No mate preference associated with the supergene controlling social organization in Alpine silver ants. *J Evol Biol*. 2019;32:742–748. <https://doi.org/10.1111/jeb.13479>.
- Banschbach VS, Herbers JM. Plasticity of social organization in a forest ant species. *Behav Ecol Sociobiol*. 1999;45:451–465. <https://doi.org/10.1007/s002650050584>.
- Blacher P *et al*. Cryptic recessive lethality of a supergene controlling social organization in ants. *Mol Ecol*. 2023;32:1062–1072. <https://doi.org/10.1111/mec.16821>.
- Blacher P, De Gasperin O, Chapuisat M. Cooperation by ant queens during colony-founding perpetuates alternative forms of social organization. *Behav Ecol Sociobiol*. 2021;75:165. <https://doi.org/10.1007/s00265-021-03105-1>.
- Boomsma JJ, Kronauer DJC, Pedersen JS. The evolution of social insect mating systems. In: *Organization of insect societies*. Harvard University Press; 2009. p. 3–25.
- Boulay R, Arnan X, Cerdá X, Retana J. The ecological benefits of larger colony size may promote polygyny in ants. *J Evol Biol*. 2014;27:2856–2863. <https://doi.org/10.1111/jeb.12515>.
- Brelsford A *et al*. An ancient and eroded social supergene is widespread across *Formica* ants. *Curr Biol*. 2020;30:304–311.e4. <https://doi.org/10.1016/j.cub.2019.11.032>.
- Buschinger A. Social parasitism among ants: a review (Hymenoptera: Formicidae). *Myrmecol News*. 2009;12: 219–235. https://doi.org/10.25849/myrmecol.news_012:219.
- Chang CC *et al*. Second-generation PLINK: rising to the challenge of larger and richer datasets. *Gigascience*. 2015;4:7. <https://doi.org/10.1186/s13742-015-0047-8>.
- Chapuisat M. Supergenes as drivers of ant evolution. *Myrmecol News*. 2023;33:1–18. https://doi.org/10.25849/MYRMECOL_NEWS_033:001.
- Choppin M *et al*. Queen and worker phenotypic traits are associated with colony composition and environment in *Temnothorax rugatulus* (Hymenoptera: Formicidae), an ant with alternative reproductive strategies. *Myrmecol News*. 2021;31:61–69. https://doi.org/10.25849/myrmecol.news_031:061.
- Crozier RH. Karyotypes of twenty-one ant species (Hymenoptera; formicidae), with reviews of the known ant karyotypes. *Can J Genet Cytol*. 1970;12:109–128. <https://doi.org/10.1139/g70-018>.
- Dahan RA, Rabeling C. Multi-queen breeding is associated with the origin of inquiline social parasitism in ants. *Sci Rep*. 2022;12:14680. <https://doi.org/10.1038/s41598-022-17595-0>.
- Danecek P *et al*. The variant call format and VCFtools. *Bioinformatics*. 2011;27:2156–2158. <https://doi.org/10.1093/bioinformatics/btr330>.
- De Gasperin O, Blacher P, Choppin M, Chapuisat M. Supergene regulation of ant social organization: a P haplotype in workers shifts colony ontogeny towards multiple queens. *Commun Biol*. 2025;8:1035. <https://doi.org/10.1038/s42003-025-08438-5>.
- Dobin A *et al*. STAR: ultrafast universal RNA-seq aligner. *Bioinformatics*. 2013;29:15–21. <https://doi.org/10.1093/bioinformatics/bts635>.
- Dudchenko O *et al*. De novo assembly of the *Aedes aegypti* genome using Hi-C yields chromosome-length scaffolds. *Science*. 2017;356:92–95. <https://doi.org/10.1126/science.aal3327>.
- Durand NC *et al*. Juicebox provides a visualization system for Hi-C contact maps with unlimited zoom. *Cell Syst*. 2016;3: 99–101. <https://doi.org/10.1016/j.cels.2015.07.012>.
- Erbii M *et al*. Evolutionary genomics of socially polymorphic populations of *Pogonomyrmex californicus*. *BMC Biol*. 2024;22:109. <https://doi.org/10.1186/s12915-024-01907-z>.
- Faria R, Navarro A. Chromosomal speciation revisited: rearranging theory with pieces of evidence. *Trends Ecol Evol*. 2010;25:660–669. <https://doi.org/10.1016/j.tree.2010.07.008>.
- Garrison E, Marth G. 2012. Haplotype-based variant detection from short-read sequencing [preprint]. *arXiv*. Available from: <http://arxiv.org/abs/1207.3907>
- Guan D *et al*. Identifying and removing haplotypic duplication in primary genome assemblies. *Bioinformatics*. 2020;36: 2896–2898. <https://doi.org/10.1093/bioinformatics/btaa025>.
- Heinze J, Keller L. Alternative reproductive strategies: a queen perspective in ants. *Trends Ecol Evol*. 2000;15:508–512. [https://doi.org/10.1016/S0169-5347\(00\)01995-9](https://doi.org/10.1016/S0169-5347(00)01995-9).
- Heinze J, Rueppell O. The frequency of multi-queen colonies increases with altitude in a Nearctic ant. *Ecol Entomol*. 2014;39: 527–529. <https://doi.org/10.1111/een.12119>.
- Helleu Q, Roux C, Ross KG, Keller L. Radiation and hybridization underpin the spread of the fire ant social supergene. *Proc Natl Acad Sci U S A*. 2022;119:e2201040119. <https://doi.org/10.1073/pnas.2201040119>.
- Herbers JM. Nest site limitation and facultative polygyny in the ant *Leptothorax longispinosus*. *Behav Ecol Sociobiol*. 1986;19: 115–122. <https://doi.org/10.1007/BF00299946>.
- Jay P *et al*. Mutation load at a mimicry supergene sheds new light on the evolution of inversion polymorphisms. *Nat Genet*. 2021;53:288–293. <https://doi.org/10.1038/s41588-020-00771-1>.
- Jongepier E *et al*. Convergent loss of chemoreceptors across independent origins of slave-making in ants. *Mol Biol Evol*. 2022;39:1–13. <https://doi.org/10.1093/molbev/msab305>.
- Kay T, Helleu Q, Keller L. Iterative evolution of supergene-based social polymorphism in ants. *Philos Trans R Soc Lond B Biol Sci*. 2022;377:20210196. <https://doi.org/10.1098/rstb.2021.0196>.
- Keller L. Social life: the paradox of multiple-queen colonies. *Trends Ecol Evol*. 1995;10:355–360. [https://doi.org/10.1016/S0169-5347\(00\)89133-8](https://doi.org/10.1016/S0169-5347(00)89133-8).
- Keller L, Ross KG. Selfish genes: a green beard in the red fire ant. *Nature*. 1998;394:573–575. <https://doi.org/10.1038/29064>.
- Kolmogorov M, Yuan J, Lin Y, Pevzner PA. Assembly of long, error-prone reads using repeat graphs. *Nat Biotechnol*. 2019;37: 540–546. <https://doi.org/10.1038/s41587-019-0072-8>.

- Krzywinski M *et al.* Circos: an information aesthetic for comparative genomics. *Genome Res.* 2009;19:1639–1645. <https://doi.org/10.1101/gr.092759.109>.
- Kundu R, Casey J, Sung W-K. 2019. HyPo: Super Fast & Accurate Polisher for Long Read Genome Assemblies [preprint]. bioRxiv:2019.12.19.882506. Available from: <https://www.biorxiv.org/content/10.1101/2019.12.19.882506v1>
- Küpper C *et al.* A supergene determines highly divergent male reproductive morphs in the ruff. *Nat Genet.* 2016;48:79–83. <https://doi.org/10.1038/ng.3443>.
- Lajmi A, Cohen P, Lee CC, Frenkel Z, Pellen Y, Privman E. Repeated evolution of supergenes on an ancient social chromosome. *Curr Biol.* 2026;36:1233–1246. <https://doi.org/10.1016/j.cub.2026.01.067>.
- Lawson LP, Vander Meer RK, Shoemaker D. Male reproductive fitness and queen polyandry are linked to variation in the supergene Gp-9 in the fire ant *Solenopsis invicta*. *Proc Biol Sci.* 2012;279:3217–3222. <https://doi.org/10.1098/rspb.2012.0315>.
- Leppänen J, Seppä P, Vepsäläinen K, Savolainen R. Genetic divergence between the sympatric queen morphs of the ant *Myrmica rubra*. *Mol Ecol.* 2015;24:2463–2476. <https://doi.org/10.1111/mec.13170>.
- Li H. Minimap2: pairwise alignment for nucleotide sequences. *Bioinformatics.* 2018;34:3094–3100. <https://doi.org/10.1093/bioinformatics/bty191>.
- Li H, Durbin R. Fast and accurate short read alignment with Burrows–Wheeler transform. *Bioinformatics.* 2009;25:1754–1760. <https://doi.org/10.1093/bioinformatics/btp324>.
- Liu H *et al.* Direct determination of the mutation rate in the bumblebee reveals evidence for weak recombination-associated mutation and an approximate rate constancy in insects. *Mol Biol Evol.* 2017;34:119–130. <https://doi.org/10.1093/molbev/msw226>.
- Martin M, Ebert P, Marschall T. Read-based phasing and analysis of phased variants with WhatsHap. *Methods Mol Biol.* 2023;2590:127–138. https://doi.org/10.1007/978-1-0716-2819-5_8.
- Mona S *et al.* Genomic evidence of a complex supergene system linking dispersal to social polymorphism. *Curr Biol.* 2025;35:6155–6162.e5. <https://doi.org/10.1016/j.cub.2025.10.065>.
- Negróni MA *et al.* Social organization and the evolution of life-history traits in two queen morphs of the ant *Temnothorax rugatulus*. *J Exp Biol.* 2021b;224:jeb232793. <https://doi.org/10.1242/jeb.232793>.
- Negróni MA, Feldmeyer B, Foitzik S. Experimental increase in fecundity causes upregulation of fecundity and body maintenance genes in the fat body of ant queens. *Biol Lett.* 2021a;17:20200909. <https://doi.org/10.1098/rsbl.2020.0909>.
- Negróni MA, Foitzik S, Feldmeyer B. Long-lived *Temnothorax* ant queens switch from investment in immunity to antioxidant production with age. *Sci Rep.* 2019;9:7270. <https://doi.org/10.1038/s41598-019-43796-1>.
- Peccoud J. STRyper: a macOS application for microsatellite genotyping and chromatogram management. *PLoS One.* 2025;20:e0318806. <https://doi.org/10.1371/journal.pone.0318806>.
- Pedersen J, Boomsma JJ. The effect of habitat saturation on the number and turnover of queens in the polygynous ant *Myrmica sulcinodis*. *J Evol Biol.* 1999;12:903–917. <https://doi.org/10.1046/j.1420-9101.1999.00109.x>.
- Plateaux L. Comparaison des cycles saisonniers, des durées des sociétés et des productions des trois espèces de fourmis *Leptothorax* (*Myrafant*) du groupe *nylanderii*. *Actes des Colloques Insectes Sociaux.* 1986;3:221–234.
- Prebus M. Insights into the evolution, biogeography and natural history of the acorn ants, genus *Temnothorax* Mayr (Hymenoptera: Formicidae). *BMC Evol Biol.* 2017;17:250. <https://doi.org/10.1186/s12862-017-1095-8>.
- Purcell J, Brelford A, Wurm Y, Perrin N, Chapuisat M. Convergent genetic architecture underlies social organization in ants. *Curr Biol.* 2014;24:2728–2732. <https://doi.org/10.1016/j.cub.2014.09.071>.
- Rajakumar R *et al.* Social regulation of a rudimentary organ generates complex worker-caste systems in ants. *Nature.* 2018;562:574–577. <https://doi.org/10.1038/s41586-018-0613-1>.
- Romiguer J *et al.* Population genomics of eusocial insects: the costs of a vertebrate-like effective population size. *J Evol Biol.* 2014;27:593–603. <https://doi.org/10.1111/jeb.12331>.
- Ross KG, Keller L. Ecology and evolution of social organization: insights from fire ants and other highly eusocial insects. *Annu Rev Ecol Syst.* 1995;26:631–656. <https://doi.org/10.1146/annurev.es.26.110195.003215>.
- Ross KG, Keller L. Genetic control of social organization in an ant. *Proc Natl Acad Sci U S A.* 1998;95:14232–14237. <https://doi.org/10.1073/pnas.95.24.14232>.
- Ross KG, Vargo EL, Keller L. Social evolution in a new environment: the case of introduced fire ants. *Proc Natl Acad Sci U S A.* 1996;93:3021–3025. <https://doi.org/10.1073/pnas.93.7.3021>.
- Rüppell O, Heinze J. Alternative reproductive tactics in females: the case of size polymorphism in winged ant queens. *Insectes Soc.* 1999;46:6–17. <https://doi.org/10.1007/s000400050106>.
- Rüppell O, Heinze J, Hölldobler B. Size-dimorphism in the queens of the North American ant *Leptothorax rugatulus* (Emery). *Insectes Soc.* 1998;45:67–77. <https://doi.org/10.1007/s000400050069>.
- Rüppell O, Heinze J, Hölldobler B. Alternative reproductive tactics in the queen-size-dimorphic ant *Leptothorax rugatulus* (Emery) and their consequences for genetic population structure. *Behav Ecol Sociobiol.* 2001a;50:189–197. <https://doi.org/10.1007/s002650100359>.
- Rüppell O, Heinze J, Hölldobler B. Complex determination of queen body size in the queen size dimorphic ant *Leptothorax rugatulus* (Formicidae: Hymenoptera). *Heredity (Edinb).* 2001b;87:33–40. <https://doi.org/10.1046/j.1365-2540.2001.00904.x>.
- Scarparo G, Palanchon M, Brelford A, Purcell J. Social antagonism facilitates supergene expansion in ants. *Curr Biol.* 2023;33:5085–5095.e4. <https://doi.org/10.1016/j.cub.2023.10.049>.
- Schär S, Nash DR. Evidence that microgynes of *Myrmica rubra* ants are social parasites that attack old host colonies. *J Evol Biol.* 2014;27:2396–2407. <https://doi.org/10.1111/jeb.12482>.
- Seppä P, Sundström L, Punttila P. Facultative polygyny and habitat succession in boreal ants. *Biol J Linn Soc Lond.* 1995;56:533–551. <https://doi.org/10.1111/j.1095-8312.1995.tb01109.x>.
- Shumate A, Salzberg SL. Liftoff: accurate mapping of gene annotations. *Bioinformatics.* 2021;37:1639–1643. <https://doi.org/10.1093/bioinformatics/btaa1016>.

- Sigeman H *et al.* A novel supergene controls queen size and colony social organization in the ant *Myrmica ruginodis*. *Mol Biol Evol.* 2025;42:msaf255. <https://doi.org/10.1093/molbev/msaf255>.
- Simão FA, Waterhouse RM, Ioannidis P, Kriventseva EV, Zdobnov EM. BUSCO: assessing genome assembly and annotation completeness with single-copy orthologs. *Bioinformatics.* 2015;31:3210–3212. <https://doi.org/10.1093/bioinformatics/btv351>.
- Stoldt M, Negroni MA, Feldmeyer B, Foitzik S. Molecular adjustment to a social niche: brain transcriptomes reveal divergent influence of social environment on the two queen morphs of the ant *Temnothorax rugatulus*. *Mol Ecol.* 2025;34:e17649. <https://doi.org/10.1111/mec.17649>.
- Vizueta J *et al.* Adaptive radiation and social evolution of the ants. *Cell.* 2025;188:4828–4848.e25. <https://doi.org/10.1016/j.cell.2025.05.030>.
- Walker SH, Lacy KD, Ross KG, Zeng H. A comprehensive account of the breeding systems of the fire ant *Solenopsis invicta*. *Ecol Evol.* 2025;15:e71888. <https://doi.org/10.1002/ece3.71888>.
- Wang J *et al.* A Y-like social chromosome causes alternative colony organization in fire ants. *Nature.* 2013;493:664–668. <https://doi.org/10.1038/nature11832>.
- Waugh AH *et al.* Molecular underpinnings of plasticity and supergene-mediated polymorphism in fire ant queens. *J Evol Biol.* 2025;38:333–344. <https://doi.org/10.1093/jeb/voae159>.
- Wheeler DE, Nijhout FH. Soldier determination in *Pheidole bicarinata*: effect of methoprene on caste and size within castes. *J Insect Physiol.* 1983;29:847–854. [https://doi.org/10.1016/0022-1910\(83\)90151-8](https://doi.org/10.1016/0022-1910(83)90151-8).
- Wiernasz DC, Cole BJ. Spatial distribution of *Pogonomyrmex occidentalis*: recruitment, mortality and overdispersion. *J Anim Ecol.* 1995;64:519. <https://doi.org/10.2307/5654>.
- Wolf JI, Seppä P. Queen size dimorphism in social insects. *Insectes Soc.* 2016;63:25–38. <https://doi.org/10.1007/s00040-015-0445-z>.
- Xu M *et al.* TGS-GapCloser: a fast and accurate gap closer for large genomes with low coverage of error-prone long reads. *Gigascience.* 2020;9:giaa094. <https://doi.org/10.1093/gigascience/giaa094>.
- Yang S *et al.* Parent-progeny sequencing indicates higher mutation rates in heterozygotes. *Nature.* 2015;523:463–467. <https://doi.org/10.1038/nature14649>.
- Zheng X *et al.* A high-performance computing toolset for relatedness and principal component analysis of SNP data. *Bioinformatics.* 2012;28:3326–3328. <https://doi.org/10.1093/bioinformatics/bts606>.